

RESEARCH LETTER

10.1029/2018GL077490

Key Points:

- We report a seismic swarm in the Bransfield Strait, Antarctica, and subsequent VT activity at Deception Island volcano
- The swarm location near Deception Island may have prompted the VT swarm by dynamic triggering of volcanic activity
- Alternatively, both the distal and local VT swarms could be a result of a magmatic intrusion at Deception Island

Supporting Information:

- Supporting Information S1

Correspondence to:

J. Almendros,
vikingo@ugr.es

Citation:

Almendros, J., Carmona, E., Jiménez, V., Díaz-Moreno, A., & Lorenzo, F. (2018). Volcano-tectonic activity at Deception Island volcano following a seismic swarm in the Bransfield Rift (2014–2015). *Geophysical Research Letters*, 45, 4788–4798. <https://doi.org/10.1029/2018GL077490>

Received 9 FEB 2018

Accepted 8 MAY 2018

Accepted article online 16 MAY 2018

Published online 30 MAY 2018

Volcano-Tectonic Activity at Deception Island Volcano Following a Seismic Swarm in the Bransfield Rift (2014–2015)

J. Almendros^{1,2} , E. Carmona¹ , V. Jiménez¹ , A. Díaz-Moreno³ , and F. Lorenzo^{1,4} 

¹Andalusian Institute of Geophysics, University of Granada, Granada, Spain, ²Department of Theoretical and Cosmos Physics, University of Granada, Granada, Spain, ³School of Environmental Sciences, University of Liverpool, Liverpool, UK, ⁴IES Martín Aldehuela, Malaga, Spain

Abstract In September 2014 there was a sharp increase in the seismic activity of the Bransfield Strait, Antarctica. More than 9,000 earthquakes with magnitudes up to 4.6 located SE of Livingston Island were detected over a period of 8 months. A few months after the series onset, local seismicity at the nearby (~35 km) Deception Island volcano increased, displaying enhanced long-period seismicity and several outbursts of volcano-tectonic (VT) earthquakes. Before February 2015, VT earthquakes occurred mainly at 5–20 km SW of Deception Island. In mid-February the numbers and sizes of VT earthquakes escalated, and their locations encompassed the whole volcanic edifice, suggesting a situation of generalized unrest. The activity continued in anomalously high levels at least until May 2015. Given the spatial and temporal coincidence, it is unlikely that the Livingston series and the Deception VT swarm were unrelated. We propose that the Livingston series may have produced a triggering effect on Deception Island volcano. Dynamic stresses associated to the seismic swarm may have induced overpressure in the unstable volcanic system, leading to a magmatic intrusion that may in turn have triggered the VT swarm. Alternatively, both the Livingston earthquakes and the VT swarm could be consequences of a magmatic intrusion at Deception Island. The Livingston series would be an example of precursory distal VT swarm, which seems to be a common feature preceding volcanic eruptions and magma intrusions in long-dormant volcanoes.

Plain Language Summary In September 2014 a seismic series occurred near Livingston Island, Bransfield Strait, Antarctica. With 9,000 earthquakes and magnitudes up to 4.6, it is the most numerous swarm ever reported in this region. In February 2015, a volcano-tectonic swarm took place at Deception Island volcano, a nearby, active volcanic system located 35 km SE. The swarm comprised several hundred earthquakes with magnitudes up to 3.2. The spatial and temporal coincidence of these two events suggests that they could be either cause and effect or consequences of a common process. We propose that the Livingston earthquakes may have induced overpressure in the volcanic system of Deception Island that could trigger the seismic swarm. Alternatively, both swarms could represent the delayed effect of a magmatic intrusion below the volcano. This relationship adds to a growing body of evidence of earthquake-volcano interactions that must be taken into account in order to properly assess volcanic hazards.

1. Introduction

The Bransfield Strait, Antarctica, is located between the Antarctic Peninsula and the South Shetland Islands (Figure 1). It is a region dominated by an extensional regime, promoted by the separation of the South Shetland microplate and the Antarctic Plate (Catalán et al., 2013; Galindo-Zaldívar et al., 2004; Maldonado et al., 2015). The Bransfield rift has a NE-SW direction, forming a series of extensional basins. Several volcanic edifices can be found along the rift, some of them subaerial and some submarine.

Deception Island is a prominent volcano of the Bransfield rift (Figure 1). It is among the most active volcanoes in Antarctica, with more than 20 eruptions documented in the last two centuries (Bartolini et al., 2014). Recent eruptions took place in 1967–1970 (e.g., Smellie, 2002). Other signs of volcanic activity include an extensive hydrothermal system, fumaroles, gas emissions, surface deformations, and a generally moderate but highly

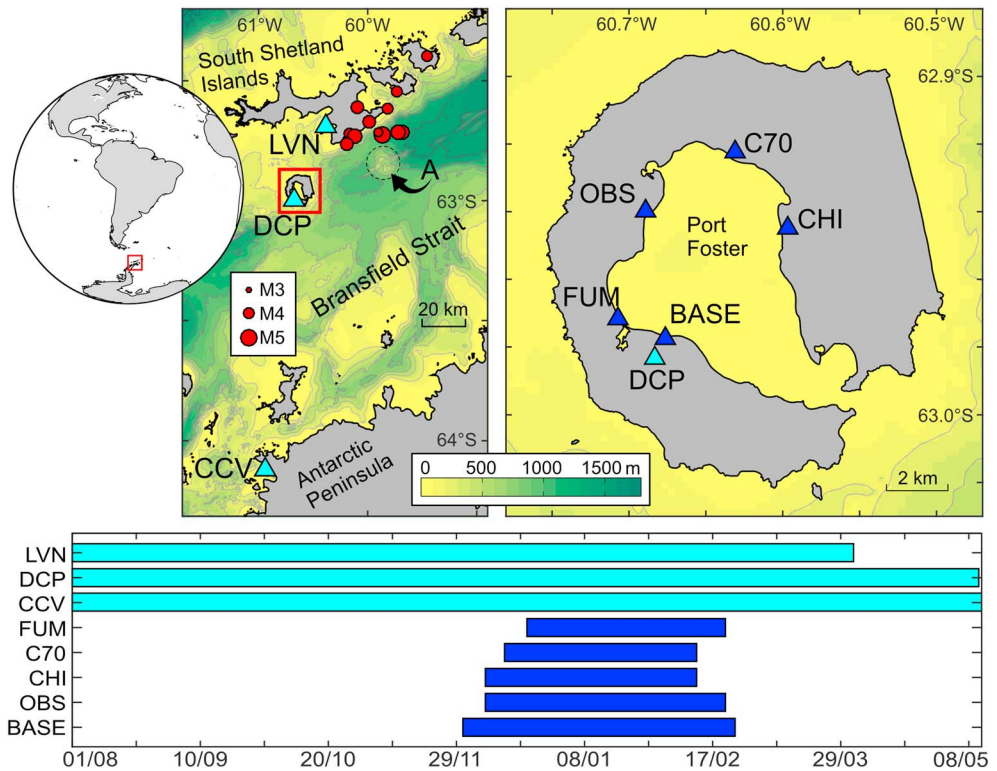


Figure 1. (top) Map of the Bransfield Strait and Deception Island, showing the locations of the seismic stations used in this study. Red squares mark the areas zoomed in the next plot. Triangles indicate seismic stations (cyan for permanent stations and blue for temporary stations). Notice that OBS is the name of a station and does not refer to an ocean bottom seismometer. Red dots in the left panel show the epicenters of earthquakes reported by the International Seismological Center (ISC, 2017) in the period 2014–2015. Bathymetry contour interval is 200 m. The dashed circle indicates a submarine volcanic feature labeled Edifice A by Gracia et al. (1996). (bottom) Operating periods of the seismic stations.

variable level of volcano seismicity (Almendros et al., 2015; Carmona et al., 2012; Ibáñez, Almendros, et al., 2003; Ortiz et al., 1997).

In the framework of the Spanish Polar Program, the Andalusian Institute of Geophysics, University of Granada (IAG-UGR), has carried out research projects at Deception Island since 1994 to investigate the seismic activity and structure of the volcano and surrounding areas (e.g., Almendros et al., 1997, 1999; Benitez et al., 2007; Carmona et al., 2010, 2012, 2014; García-Yeguas et al., 2011; Ibáñez, Almendros, et al., 2003; Ibáñez, Carmona, et al., 2003; Ibáñez et al., 1997, 2000, 2017; Jiménez et al., 2017; Luzón et al., 2011; Prudencio et al., 2013, 2015; Zandomeneghi et al., 2009). The IAG-UGR also monitors the seismic activity of Deception Island volcano and provides scientific advice for the management of the volcanic alert system. Seismic monitoring is based on a temporary seismic network deployed generally from December to February, coinciding with the operation of the Gabriel de Castilla Base. Moreover, since 2008 three permanent broadband stations are maintained in the region, at Cierva Cove, Deception Island, and Livingston Island (Carmona et al., 2014).

Two major seismic crises have been reported since 1986, when seismic monitoring was reestablished at Deception Island after the 1967–1970 eruptions. They occurred in 1992 (Ortiz et al., 1997) and 1999 (Ibáñez, Carmona, et al., 2003) and were characterized by a sharp increase in the number and magnitude of volcano-tectonic (VT) earthquakes, reaching rates of tens of earthquakes per day and maximum magnitudes around 3. They have been interpreted as consequences of aborted magmatic intrusions.

After 1999, the seismic activity was relatively quiet, with a general dominance of long-period (LP) seismicity and occasional bursts of LP seismic activity, for example, in the 2003–2004 and the 2012–2013 surveys (Almendros et al., 2015; Carmona et al., 2012).

This behavior changed drastically in the 2014–2015 survey, when a very large number of earthquakes of tectonic and volcanic origin were detected. The number of events was 1 order of magnitude larger than the sum

of all earthquakes recorded in the previous 15 years. During the survey, data from the temporary seismic network were preliminarily analyzed in near real time. LP seismicity was unusually frequent and intense. Tectonic and VT earthquakes also occurred in large numbers. In the last weeks of the survey, the number of local earthquakes at Deception Island escalated. At the same time, LP seismicity became conspicuous, displaying increasingly larger and more recurrent LP events and tremor episodes. These observations, in the context of extensive seismo-volcanic activity, led to a change in the volcanic alert system. The Spanish Polar Committee established the volcanic alert level at yellow (enhanced monitoring to corroborate the observed anomalies) for a few days in February 2015 (Almendros et al., 2015).

In the present work we analyze the seismicity of Deception Island and surrounding areas during the period August 2014 to May 2015, using both temporary and permanent stations. We investigate the spatial and temporal evolution of the seismicity and assess the possible interactions with the activity of Deception Island volcano.

2. Instruments

Since February 2008 the IAG-UGR maintains three permanent seismic stations (LVN, DCP, and CCV; see Figure 1) at Livingston Island, Deception Island, and Cierva Cove (Carmona et al., 2014; Jiménez et al., 2017). Additionally, from December 2014 to February 2015 a temporary network composed of five short-period seismic stations (Abril, 2007; Carmona et al., 2014; Havskov & Alguacil, 2016; Weber et al., 2007) was set up at accessible areas around Port Foster (Figure 1). For further details about these instruments, see supporting information Text S1.

3. Data Analysis and Results

We analyze the seismic activity in the Bransfield Strait area during the period August 2014 to May 2015. We combine data with different spatial and temporal coverages: (1) permanent stations with a sparse spatial distribution but continuous recording (Almendros et al., 2018a) and (2) temporary stations with a dense spatial coverage of Deception Island volcano, operating between December 2014 and February 2015 (Almendros et al., 2018b). The details of the earthquake detection and location procedures are described in the supporting information Text S2 (Carmona et al., 2014; Havskov et al., 2003; Havskov & Ottemoller, 1999, 2010; Ibáñez et al., 2000; Lienert & Havskov, 1995; Luzón et al., 2011; Utheim et al., 2014; Vassallo et al., 2012; Zandomeneghi et al., 2009).

3.1. Permanent Station Data

The permanent station data reveal the occurrence of a seismic swarm comprising several thousand earthquakes in a time frame of a few months. *P* and *S* arrival times were obtained for 9,526, 2,535, and 513 earthquake records at LVN, DCP, and CCV, respectively. Some earthquakes are large enough to be included in global catalogs (see Figure 1).

In most cases, earthquake amplitudes were largest and *S-P* delays shortest at station LVN. Thus, the main focus of earthquake activity was closest to Livingston Island. Most earthquakes have *S-P* delays in the range 2.9–3.5 s at LVN (Figure 2a). Some of these earthquakes were also detected at DCP, with smaller amplitudes and *S-P* delays of 6.9–7.5 s (Figure 2b, blue). Only the largest earthquakes were detected at CCV, with *S-P* times of ~19.5 s. Estimated magnitudes range up to 4.6 and are characterized by a *b* parameter of ~1 (Figures S1 and S2). There is no dominant earthquake, and there are 12 events with magnitudes above 4.0, mostly during September. The total seismic moment is $7.8 \cdot 10^{16}$ N·m, equivalent to a magnitude 5.2 earthquake.

The seismic activity began with two short-lived pulses of small-magnitude earthquakes on 15 and 22 August 2014. On 31 August, the number of earthquakes increased again and remained very high for about a month. This is the most intense period of the swarm, in terms of earthquake rates and seismic moment. By 4 October, the series had already produced 50% of the earthquakes and 87% of the total moment release. Earthquake rates diminished slowly during the following 6 months, with some irregular bursts on 15 October, 24 November, and 20 December 2014. Station LVN stopped functioning on 1 April 2015, although by that time the series had practically faded out.

At DCP, several earthquakes belonging to the Livingston series have been detected (blue dots in Figure 2b). Nevertheless, there are also earthquakes characterized by smaller *S-P* times, in a broad range spanning 1–5 s

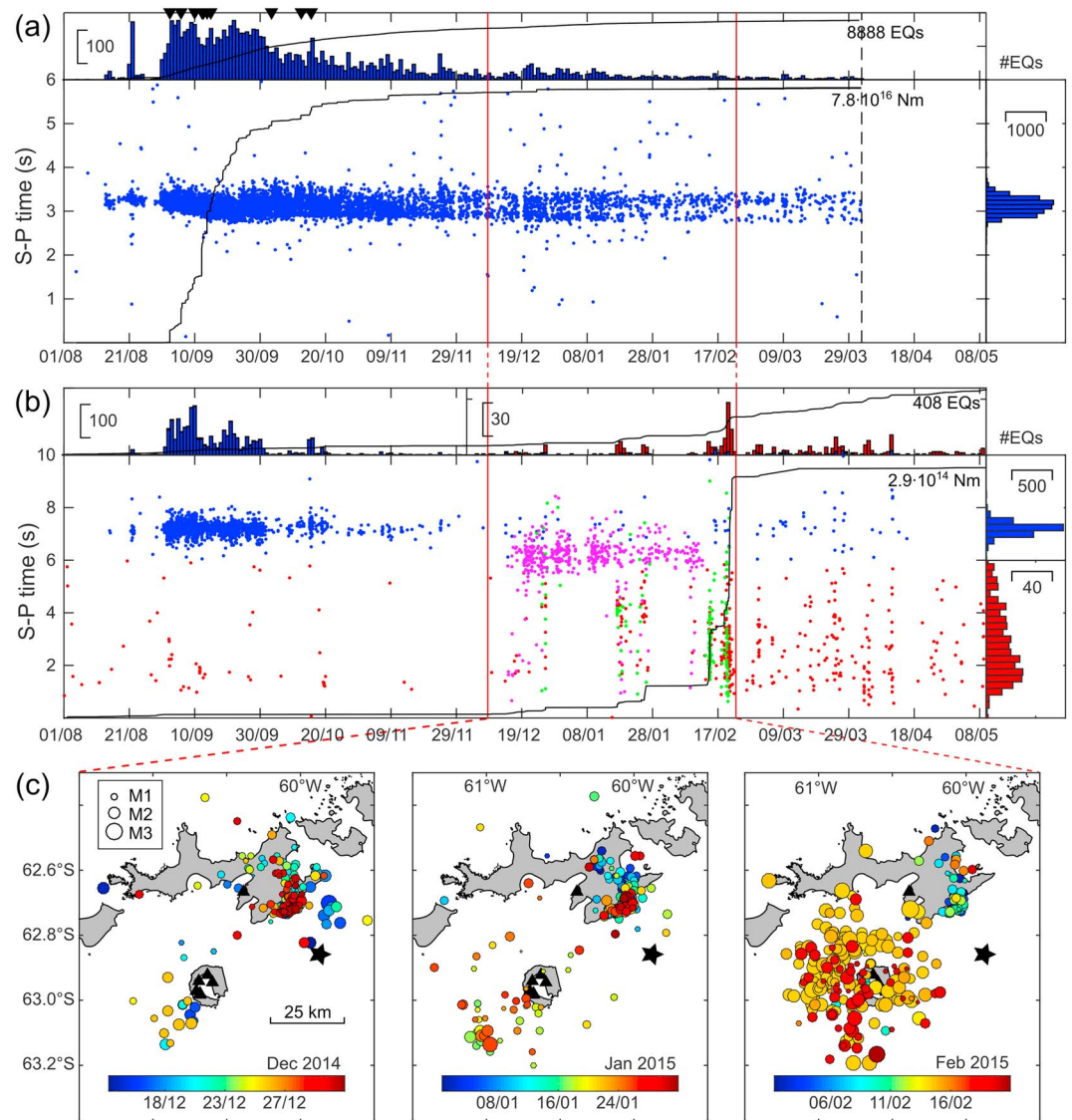


Figure 2. (a) *S-P* times at station LVN during the period August 2014 to May 2015. The panels show the *S-P* delays versus time (center), the daily number of earthquakes (top), and the *S-P* time distribution, with a bin width of 0.25 s (right). A dashed line marks the end of the recording period. Inverted triangles denote 12 earthquakes reported by ISC. Red vertical lines indicate the span of the temporary network operations. Black lines show the evolution of the number of earthquakes (top) and cumulative seismic moment (center). Same as (a) for station DCP. Colors identify local ($t_{sp} < 6$ s, red) and distant ($t_{sp} > 6$ s, blue) earthquakes. Green and magenta dots correspond to OBS and C70, respectively. Black lines displaying the evolution of the earthquake number and moment are calculated using VT earthquakes only (red dots). Note the change in scale in the histograms for times after 1 December and *S-P* times below 6 s. (c) Epicenter locations in December (left), January (middle), and February (right). Dot colors are coded by time, and dot sizes are scaled by magnitude. Triangles indicate station locations. The black star marks the position of the submarine volcano Edifice A (see Figure 1). ISC = International Seismological Center; VT = volcano-tectonic.

(red dots in Figure 2b). The small *S-P* times indicate that they are local, VT earthquakes, occurring within the volcanic edifice of Deception Island. *P* and *S* arrivals for 408 VT earthquakes were identified, although many other earthquakes were too small for reliable phase identification. This number is small compared to the activity recorded at Livingston Island. However, these events are highly significant, because they may represent a seismic reactivation of the volcano.

VT earthquakes occurred sporadically up to early December. Later on, they tended to occur more frequently and were grouped in clusters (e.g., 25 December 2014, 17–19 and 25–26 January 2015, and 13–14 and 18–21 February 2015). The highest magnitudes occurred in late February (Figures 2b and S3). The activity continued

through March and April, with two clusters (2–5 and 9–12 April) displaying even lower *S-P* delays. This indicates events located near or within the Deception Island caldera. The seismic activity decayed by the end of the recording period (10 May 2015). However, although the magnitudes are low, the number of earthquakes is still relevant, and we cannot establish precisely how long this series may have continued.

3.2. Temporary Network Data

Basic location capabilities were maintained from 8 December to 22 February (red lines in Figure 2). In this period, the network detected a part of the Livingston Island series and several bursts of local VT seismicity at Deception Island volcano (Figure 2b). Very often VT earthquakes were very small and could be detected only at the closest stations. Therefore, they cannot be located, although they can be counted and their *S-P* times measured to have a rough idea of their temporal and spatial distribution. For example, green and magenta dots in Figure 2b correspond to VT earthquakes at station OBS and C70. It can be noticed that the 13–14 February cluster is most active at OBS, and thus its source should be closest to OBS. Similarly, at C70 there is more activity in the December and January clusters. Since C70 is closer to Livingston, more Livingston swarm earthquakes are detected, with slightly smaller *S-P* times (~ 6 s).

Figure 2c shows the results of the source location procedure. A total of 835 earthquakes have been located, and several features of the spatial and temporal distribution of the earthquakes can be noticed. For example, there is a relevant seismogenetic zone located near the eastern tip of Livingston Island at about 62.7°S , 60.0°W . This area comprised $\sim 50\%$ of the located earthquakes, with magnitudes in the range 1.0–2.0, and was active during the whole summer survey (December–February). The distribution of earthquakes around Deception Island is more irregular. In December, there were just a few earthquakes scattered toward the SW. Most of them occur around 25 December. In January, a few low-magnitude earthquakes were located around Deception. There was also a small cluster ~ 20 km SW of Deception, comprising the earthquakes occurring in 17–19 and 25–26 January. But in February the situation changed. First, there were many more earthquakes near Deception Island volcano, close to or within the caldera. Second, the epicenters encompassed the complete volcanic edifice. Finally, many earthquakes have large magnitudes of up to 3.2. Most of these earthquakes occurred in two clusters, on 13–14 and 18–21 February.

Calculated earthquake depths are mostly limited to the first 10 km of the crust, although a few solutions suggest the presence of deeper sources, down to 20–25 km, both in the Livingston cluster and near Deception Island volcano. Therefore, these earthquakes seem to occur in the shallow crust. However, the depth resolution is limited due to the irregular station coverage, and further interpretations should be avoided.

4. Discussion

4.1. The 2014–2015 Livingston Seismic Swarm

The Bransfield Strait is an area of active seismicity. Despite the poor permanent station coverage, the International Seismological Center (ISC) catalog (ISC, 2017) comprises ~ 200 earthquakes with magnitudes above ~ 4.0 since 1960. In the past decades, a few detailed studies have revealed a significant background of low-magnitude microseismicity around the Bransfield rift (Dziak et al., 2010; Ibáñez et al., 1997; Pelayo & Wiens, 1989; Robertson-Maurice et al., 2003). Most earthquakes are shallow (< 10 km), but intermediate-depth earthquakes have been also identified (Ibáñez et al., 1997; Robertson-Maurice et al., 2003). They are interpreted as a consequence of the subduction of the Drake plate under the South Shetland continental block.

The seismicity of the Bransfield Strait often takes the form of spatiotemporal clusters (Dziak et al., 2010; Ibáñez, Carmona, et al., 2003; Robertson-Maurice et al., 2003). They are localized near volcanic features, including not only volcanic islands such as Bridgeman and Deception but also submarine structures such as Orca volcano and other fissure-like ridges. The close relationship between seismic swarms and volcanic structures suggests that these earthquakes could be originated by ongoing magmatic activity (Dziak et al., 2010; Robertson-Maurice et al., 2003).

In this context, our data demonstrate the occurrence of an intense seismic swarm near Livingston Island in 2014–2015. It is the most numerous swarm ever reported in the Bransfield area, comprising $\sim 9,000$ earthquakes detected along a period of 8 months. The swarm started in early September 2014, following some precursory seismicity in August. The largest earthquakes (up to magnitude 4.6) and earthquake rates (up to ~ 180 events per day) took place in the early stages of the series (September–October). There were two phases of maximum earthquake production during September, although large earthquakes were also recorded

in October. After September, the number of earthquakes decayed slowly with time, with occasional bursts of activity (Figure 2). The seismicity lasted for 8 months, until it faded out in April–May 2015. The operation of a seismic network at Deception Island during 2.5 months (Figure 1) allowed for the location of a small part of the series. The results identify a source region near the eastern tip of Livingston Island (Figure 2c). Given the stability of the S - P times displayed in Figure 2, we hypothesize that this is also the source region of the whole Livingston series. The small variability of the S - P delays also suggests that the earthquakes occurred within a spatially limited source area.

The Livingston swarm could be originated either by tectonic stresses acting on the shallow crust, due to the opening of the Bransfield Rift, or by instabilities caused by a localized magmatic intrusion. Both processes are likely to happen in that area off Livingston Island. On the one hand, the region is under an extensional tectonic regime. Geodetic studies have shown that the Antarctic Peninsula and the South Shetland Islands are moving apart at a rate of 7–10 mm/year (Berrocoso et al., 2016; Dietrich et al., 2004). Thus, the occurrence of series of tectonic earthquakes is expected, similar to those produced at other oceanic ridges (e.g., Rundquist & Sobolev, 2002). On the other hand, the region displays active volcanism (LeMasurier & Thomson, 1990). Earthquake swarms generally occur near volcanic structures, which suggests that most of them may have a volcanic origin (Dziak et al., 2010; Ibáñez, Carmona, et al., 2003; Robertson-Maurice et al., 2003). The presence of shallow magma reservoirs along the Bransfield Rift is also supported by results from seismic profiles (Barker & Austin, 1998; Christeson et al., 2003; Grad et al., 1997), seismic tomography (Ben-Zvi et al., 2009; Zandomenighi et al., 2009), magnetotelluric data (Pedrera et al., 2012), and gravity and magnetic surveys (Catalán et al., 2013, 2014).

The b parameter of the series, near 1, seems to favor a tectonic origin. It is generally accepted that volcanic sequences have a larger b parameter; however, there are many exceptions to this rule (Roberts et al., 2015), and therefore this observation does not completely exclude a volcanic origin.

Nevertheless, the duration of the Livingston swarm is very long and displays a relatively slow decay of the earthquake rates (Figure 2a). In general, tectonic series responding to a mainshock-aftershock sequence show a faster decay in the number of earthquakes. They usually follow the modified Omori law, with p values between 0.7 and 1.5 and c values of a small fraction of a day (e.g., Kisslinger & Jones, 1991; Utsu et al., 1995). In our case, a good fit between the earthquake rates and the modified Omori law cannot be found. This suggests that the Livingston swarm is not a mainshock-aftershock series responding to the reaccommodation of the stress field after a large fracture event. Instead, it may be a continuous process involving heat and fluid flow within the shallow crust in the source region, induced by magmatic activity. A similar result was obtained for the June 1999 seismic sequence of the Endeavour Segment of the Juan de Fuca Ridge (Bohnenstiehl et al., 2002, 2004). The anomalously large number of earthquakes, long duration of the series, and absence of a clearly dominant mainshock were interpreted as a demonstration of the volcanic origin of the series.

Another indication comes from the variations in the S - P times observed in Figure 2. First, there is a slight drift in the S - P times at the beginning of the series (Figure 2a). At the series onset, earthquakes have S - P times near 3.2 s that reduce gradually to \sim 2.9 s in late September. No equivalent changes are observed at DCP. Second, there is a splitting of the S - P times, starting in late October, with average values around 2.9 and 3.2 s. This can be also observed in the data from C70 (Figure 2b). The first observation suggests a propagation of the source that becomes slightly closer to LVN with time. Source migration could be explained by multiple phenomena, including fault propagation, diffusive processes, and fluid and magma motions (Battaglia et al., 2005; Bonaccorso et al., 2013; Díaz-Moreno et al., 2015; Saccorotti et al., 2002). The second observation implies the simultaneous activation of two nearby sources. This is not common in tectonic sequences and would suggest the interplay with hydrothermal or volcanic fluids.

Finally, it is remarkable that the swarm location is apparently unrelated to any volcanic structure. Detailed analyses of the bathymetry show the presence of normal faults in the source region, aligned with the Bransfield rift (Barclay et al., 2009), while the closest volcanic structure is further south (Gracia et al., 1996). However, the location uncertainties must be considered. Moreover, we have used a simple layered model based on the Deception Island structure. There are evidences that the seismic velocity in the South Shetland continental block is faster than near the rift (Ben-Zvi et al., 2009; Zandomenighi et al., 2009). Therefore, if the source-LVN path were faster than the source-DCP path, the source might be actually located further from LVN than imaged in Figure 2c. This could place the source closer to Edifice A, which could be held responsible for the earthquake swarm.

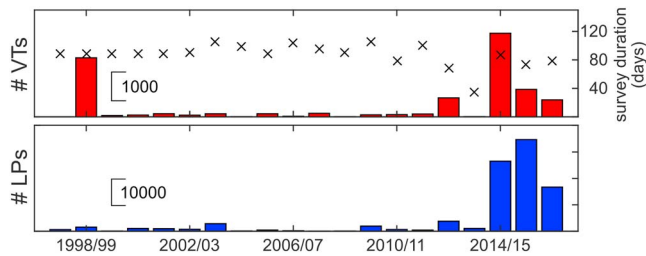


Figure 3. Total number of VTs (red) and LPs (blue) recorded during the temporary seismic surveys carried out between 1997 and 2017. Event counts were performed at stations CHI and OBS, respectively. The number of VTs includes many earthquakes that are too small to be located. Crosses in the top panel indicate the durations of the surveys in the scale shown by the right-hand y axis. VTs = volcano-tectonic earthquakes; LPs = long-period events.

4.2. Relationship With the VT Swarm at Deception Island Volcano

Exceptionally intense VT activity occurred at Deception Island volcano a few months after the onset of the 2014–2015 Livingston swarm. Source locations encompass the whole volcanic edifice, revealing a situation of generalized unrest.

This episode of VT seismicity is similar to those reported in 1992 and 1999 (Carmona et al., 2012; Ibáñez, Almendros, et al., 2003; Ibáñez, Carmona, et al., 2003; Ortiz et al., 1997). In 1992, 776 earthquakes were recorded in 2 months, with a maximum magnitude of 3.4, including four felt earthquakes (Ortiz et al., 1997). In 1999, 2,072 VT earthquakes were recorded during 2 months, with maximum rates of 80 earthquakes per day and maximum magnitude of 3.4, including two felt earthquakes (Ibáñez, Carmona et al., 2003). In 2015, a few thousand earthquakes are reported over a period of 5 months (Almendros et al., 2015), although most of them are too small to be identified at more than one station. About 400 VT earth-

quakes have been located, with maximum rates of 45 earthquakes per day and a maximum magnitude of 3.2. Thus, we could hypothesize that the 2015 VT swarm may be also related to the stress changes induced by a magmatic intrusion at shallow depths, as proposed for the other two episodes (Ibáñez, Carmona et al., 2003; Ortiz et al., 1997).

However, there are two noticeable differences. On the one hand, the 1992 and 1999 series died off after a few months. The seismicity levels at Deception Island volcano after the 2015 swarm have been anomalously high, not only during the swarm itself but during the following years as well. Figure 3 shows the total numbers of VT earthquakes and LP events reported during summer surveys from 1998 to 2017. The network configuration and detection capabilities have been basically the same since 2001 (Carmona et al., 2014), and therefore these numbers are readily comparable. The activity increased in 2015 and has continued in anomalous levels also in the 2015–2016 and 2016–2017 surveys, although it seems to be decaying back to normal thresholds. On the other hand, seismic activity during the 1992 and 1999 episodes was localized solely at Deception Island. The 2015 VT activity occurred after the largest seismic swarm (in terms of number of earthquakes and earthquake rates) ever reported in the Bransfield area. Given the relatively close temporal and spatial coincidence, it is unlikely that these two events could be completely unrelated.

Deception Island is a highly fractured volcanic edifice with an extensive hydrothermal system (e.g., Carmona et al., 2010; Martí et al., 2013; Ortiz et al., 1997) in an unstable state, as revealed, for example, by the VT series described above and the conspicuous presence of LP seismicity (Carmona et al., 2012, 2014). In the last years, this instability seems to be increasing. For example, there are evidences that pressure variations related to high-amplitude microtremors are able to trigger long-duration tremors (Jiménez et al., 2017) and induce regular series of LP events (Stich et al., 2011), which had not been observed before. Moreover, Jiménez et al. (2017) noticed that between 2012 and 2014 the number and durations of volcanic tremors at Deception Island had been growing steadily. In this scenario, the occurrence of the Livingston swarm could have had a triggering effect on Deception Island volcano.

Earthquake-generated dynamic stresses traveling as seismic waves are capable of triggering additional earthquakes at remote, critically stressed faults (see Hill & Prejean, 2015, and references therein). Triggering is not always immediate, and time delays of hours to days are common (Brodsky & van der Elst, 2014; Freed, 2005). Similarly, static and dynamic strains produced by earthquakes can induce pressure changes in distant magma bodies. In certain situations, these pressure variations might drive volcanic activity, including seismic swarms, enhanced gas emissions, thermal anomalies, deformation, and even volcanic eruptions (Aiken & Peng, 2014; Bonali, 2013; Bonali et al., 2013; Gabrieli et al., 2015; Harris & Ripepe, 2007; Hill et al., 2002; Johnston et al., 2004; Lemarchand & Grasso, 2007; Linde & Sacks, 1998; Manga & Brodsky, 2006; Marzocchi, 2002; Nishimura, 2017; Walter et al., 2007, 2009). For earthquake-volcano interactions, longer time delays are reported, ranging up to several years (Marzocchi, 2002; Nishimura, 2017). Proposed mechanisms include triggering by frictional failure, where dynamic stresses can be large enough to exceed the frictional strength of faults, and triggering through excitation of crustal fluids, where dynamic strains are thought to induce fluid transport and changes in pore pressure, reducing the effective normal stress in the fault plane and lowering the threshold required for failure (e.g., Brodsky & Prejean, 2005; Brodsky & van der Elst, 2014; Hill & Prejean, 2015).

Additional mechanisms focusing on the interactions with magmatic and hydrothermal fluids include the rectified diffusion and advective overpressure models, enhanced bubble nucleation in a supersaturated magma, and detachment and sinking of crystal-rich aggregates (Brodsky et al., 1998; Hill et al., 2002; Hill & Prejean, 2015; Manga & Brodsky, 2006).

In our case, a direct dynamic triggering of the VT earthquakes by the Livingston swarm can be ruled out, given the long delay between the start of the Livingston series and the seismicity at Deception Island (e.g., Brodsky & van der Elst, 2014; Freed, 2005; Hill, 2008; Hill et al., 1993; Prejean et al., 2004; Steacy et al., 2005). Maximum peak dynamic strains at Deception Island are on the order of 10^{-6} – 10^{-7} (Hill et al., 1993; Shearer, 2009), which exceed the triggering thresholds reported in some cases (e.g., van der Elst & Brodsky, 2010; Walter et al., 2007). We hypothesize that these strains may have induced pressure variations in the Deception Island volcanic system, by some of the mechanisms described above. In due time (months), the critically pressurized magma could build up sufficient overpressure to trigger a response in the form of a magmatic intrusion (Hill et al., 2002; Hill & Prejean, 2015; Manga & Brodsky, 2006). Static stress changes would then affect the brittle regions of the volcanic edifice and generate the VT swarm.

Alternatively, the Livingston swarm and the VT activity at Deception Island can both be consequences of magmatic processes taking place at the volcano. However, the notion that the most distant swarm starts months before the local seismicity at the volcano seems largely counterintuitive. Nevertheless, White and McCausland (2016) demonstrate that distal VT swarms located at distances of 2–40 km are usually the earliest precursors preceding volcanic eruptions in long-dormant volcanoes. These earthquakes have a swarm-like nature and start days to years prior to the magmatic eruptions. White and McCausland (2016) also report magmatic intrusions preceded by distal VT earthquake swarms and infer an empirical relationship between the cumulative seismic moment and the intruded volume. In order to justify why distal VT seismicity precedes volcanic activity, Coulon et al. (2017) simulated the propagation of heat and pressure pulses through the volcanic hydrothermal system. Their results show that even with modest horizontal/vertical anisotropy, pressure changes associated with a magmatic intrusion can affect distal regions before significant effects are produced in the volcanic edifice.

Therefore, the 2014–2015 Livingston swarm could be another example of a distal VT swarm accompanying a magmatic intrusion at Deception Island volcano. Pressure pulses would propagate laterally, reaching the region SE of Livingston Island, where the interaction with critically stressed faults may have produced the seismic swarm. Local VT earthquakes and LP seismicity at Deception Island were initiated later, when the pressure pulses reached the shallower levels of the volcanic edifice. The volume-moment relationship of White and McCausland (2016) implies that the volume intruded is $\sim 5 \cdot 10^7$ m³.

These two models assess the relationship between the Livingston swarm and the VT activity at Deception Island volcano. They share a common feature: the occurrence of a magmatic intrusion beneath Deception Island volcano that originates the local VT activity. This mechanism was also proposed for the 1992 and 1999 seismic swarms (Ibáñez, Almendros, et al., 2003; Ibáñez, Carmona, et al., 2003; Ortiz et al., 1997). The models differ in considering the Livingston swarm as a cause or an effect of the intrusion. The main drawbacks are, respectively, the small magnitudes of the Livingston earthquakes and the absence of distal VT swarms in 1992 and 1999. In any case, these interpretations suggest that Deception Island is in a highly susceptible and unstable state and confirm the dynamic interactions that can be expected at an active volcanic system. The results also underline the importance of seismic monitoring at Deception Island to provide quantitative bases for volcanic hazards assessment.

References

- Abril, M. (2007). Evolución, Diseño Y Desarrollo De Antenas Sísmicas. Las Antenas Del Gran Sasso, Del Vesubio Y Las Nuevas Antenas Sísmicas Portátiles Del Instituto Andaluz De Geofísica. Aplicación a Zonas Tectónicas Y Volcánicas (PhD thesis). University of Granada, Spain.
- Aiken, C., & Peng, Z. (2014). Dynamic triggering of microearthquakes in three geothermal/volcanic regions of California. *Journal of Geophysical Research: Solid Earth*, 119, 6992–7009. <https://doi.org/10.1002/2014JB011218>
- Almendros, J., Carmona, E., Aguí, J. F., Moreno, J., Martos, A., Alguacil, G., et al. (2018a). Seismic stations at the Bransfield Strait, Antarctica, 2014–2015. *Australian Antarctic Data Centre*. <https://doi.org/10.4225/15/5ac56ba111460>
- Almendros, J., Carmona, E., Aguí, J. F., Moreno, J., Martos, A., Alguacil, G., et al. (2018b). Seismic network at Deception Island volcano, Antarctica, 2014–2015. *Australian Antarctic Data Centre*. <https://doi.org/10.4225/15/5ac5681e2f528>
- Almendros, J., Carmona, E., Jiménez, V., Díaz-Moreno, A., Lorenzo, F., Berrocoso, M., et al. (2015). Deception Island (Antarctica): Sustained deformation and large increase in seismic activity during 2014–2015. In E. Venzke (Ed.), *Bulletin of the Global Volcanism Network* (Vol. 40). Washington, DC: Smithsonian Institution.

Acknowledgments

This work was partially funded by the Spanish Ministry of Economy through projects POL2006-08663, CTM2009-08085, CTM2010-11740, and CTM2011-16049 and by the Assignment IGME-1198 for Supporting Activities to the Spanish Polar Committee. Additional support comes from project CTM2016-77315-R. The work of A. Díaz-Moreno has been partially supported also by the NERC grant NE/P00105X/1 and project TEC2015-68752. We are grateful to the Spanish Army, Spanish Navy, and Marine Technology Unit of the Spanish Council for Scientific Research for providing logistical support and to all collaborators in the field works. Comments by G. Hayes, D. Bohnenstiehl, and D. Hill have contributed to improve the manuscript and are greatly appreciated. Raw seismic data are available at the Australian Antarctic Data Center (<https://data.aad.gov.au>) with DOIs <https://doi.org/10.4225/15/5ac56ba111460> and <https://doi.org/10.4225/15/5ac5681e2f528> for permanent stations and temporary network data, respectively (Almendros et al., 2018a, 2018b). Bathymetry data were obtained from the Global Multi-Resolution Topography project (Ryan et al., 2009) of the Interdisciplinary Earth Data Alliance (<https://www.gmrt.org>). Antarctic coastline data come from the SCAR Antarctic Digital Database (<http://www.add.scar.org>). Epicenter data were obtained from the International Seismological Center (<http://www.isc.ac.uk>).

- Almendros, J., Ibáñez, J. M., Alguacil, G., & Del Pezzo, E. (1999). Array analysis using circular-wave-front geometry: An application to locate the nearby seismo-volcanic source. *Geophysical Journal International*, 136(1), 159–170. <https://doi.org/10.1046/j.1365-246X.1999.00699.x>
- Almendros, J., Ibáñez, J. M., Alguacil, G., Del Pezzo, E., & Ortiz, R. (1997). Array tracking of the volcanic tremor source at Deception Island, Antarctica. *Geophysical Research Letters*, 24(23), 3069–3072. <https://doi.org/10.1029/97GL03096>
- Barclay, A. H., Wilcock, W. S. D., & Ibáñez, J. M. (2009). Bathymetric constraints on the tectonic and volcanic evolution of Deception Island volcano, South Shetland Islands. *Antarctic Science*, 21, 153–167. <https://doi.org/10.1017/S0954102008001673>
- Barker, D. H. N., & Austin, J. A. (1998). Rift propagation, detachment faulting, and associated magmatism in Bransfield Strait, Antarctic Peninsula. *Journal of Geophysical Research*, 103(B10), 24,017–24,043. <https://doi.org/10.1029/98JB01117>
- Bartolini, S., Geyer, A., Martí, J., Pedrazzi, D., & Aguirre-Díaz, G. (2014). Volcanic hazard on Deception Island (South Shetland Islands, Antarctica). *Journal of Volcanology and Geothermal Research*, 285, 150–168. <https://doi.org/10.1016/j.jvolgeores.2014.08.009>
- Battaglia, J., Ferrazzini, V., Staudacher, T., Aki, K., & Cheminee, J.-L. (2005). Pre-eruptive migration of earthquakes at the Piton de la Fournaise volcano (Reunion Island). *Geophysical Journal International*, 161(2), 549–558. <https://doi.org/10.1111/j.1365-246X.2005.02606.x>
- Ben-Zvi, T., Wilcock, W. S. D., Barclay, A. H., Zandomenighi, D., Ibáñez, J. M., & Almendros, J. (2009). The P-wave velocity structure of Deception Island, Antarctica, from two-dimensional seismic tomography. *Journal of Volcanology and Geothermal Research*, 180, 67–80. <https://doi.org/10.1016/j.jvolgeores.2008.11.020>
- Benitez, M. C., Ramírez, J., Segura, J. C., Ibáñez, J. M., Almendros, J., García-Yeguas, A., & Cortés, G. (2007). Continuous HMM-based seismic-event classification at Deception Island, Antarctica. *IEEE Transactions on Geoscience and Remote Sensing*, 45(1), 138–146. <https://doi.org/10.1109/TGRS.2006.882264>
- Berrococo, M., Fernández-Ros, A., Prates, G., García, A., & Kraus, S. (2016). Geodetic implications on block formation and geodynamic domains in the South Shetland Islands, Antarctic Peninsula. *Tectonophysics*, 666, 211–219. <https://doi.org/10.1016/j.tecto.2015.10.023>
- Bohnenstiehl, D. R., Dziak, R. P., Tolstoy, M., Fox, C. G., & Fowler, M. (2004). Temporal and spatial history of the 1999–2000 Endeavour Segment seismic series, Juan de Fuca Ridge. *Geochemistry, Geophysics, Geosystems*, 5, Q09003. <https://doi.org/10.1029/2004GC000735>
- Bohnenstiehl, D., Tolstoy, M., Dziak, R., Fox, C., & Smith, D. (2002). Aftershock sequences in the mid-ocean ridge environment: An analysis using hydroacoustic data. *Tectonophysics*, 354(1), 49–70. [https://doi.org/10.1016/S0040-1951\(02\)00289-5](https://doi.org/10.1016/S0040-1951(02)00289-5)
- Bonaccorso, A., Currenti, G., & Del Negro, C. (2013). Interaction of volcano-tectonic fault with magma storage, intrusion and flank instability: A thirty years study at Mt. Etna volcano. *Journal of Volcanology and Geothermal Research*, 251, 127–136. <https://doi.org/10.1016/j.jvolgeores.2012.06.002>
- Bonali, F. L. (2013). Earthquake-induced static stress change on magma pathway in promoting the 2012 Copahue eruption. *Tectonophysics*, 608, 127–137. <https://doi.org/10.1016/j.tecto.2013.10.006>
- Bonali, F. L., Tibaldi, A., Corazzato, C., Tormey, D. R., & Lara, L. E. (2013). Quantifying the effect of large earthquakes in promoting eruptions due to stress changes on magma pathway: The Chile case. *Tectonophysics*, 583, 54–67. <https://doi.org/10.1016/j.tecto.2012.10.025>
- Brodsky, E. E., & Prejean, S. G. (2005). New constraints on mechanisms of remotely triggered seismicity at Long Valley caldera. *Journal of Geophysical Research*, 110, B04302. <https://doi.org/10.1029/2004JB003211>
- Brodsky, E. E., Sturtevant, B., & Kanamori, H. (1998). Earthquakes, volcanoes, and rectified diffusion. *Journal of Geophysical Research*, 103(B10), 23,827–23,838. <https://doi.org/10.1029/98JB02130>
- Brodsky, E. E., & van der Elst, N. J. (2014). The uses of dynamic earthquake triggering. *Annual Review of Earth and Planetary Sciences*, 42(1), 317–339. <https://doi.org/10.1146/annurev-earth-060313-054648>
- Carmona, E., Almendros, J., Martín, R., Cortés, G., Alguacil, G., Moreno, J., et al. (2014). Advances in seismic monitoring at Deception Island volcano (Antarctica) since the International Polar Year. *Annals of Geophysics*, 57(3), S50321. <https://doi.org/10.4401/ag-6378>
- Carmona, E., Almendros, J., Martín, R., Serrano, I., Stich, D., & Ibáñez, J. M. (2012). Results of seismic monitoring surveys of Deception Island volcano, Antarctica, from 1999–2011. *Antarctic Science*, 24, 485–499. <https://doi.org/10.1017/S0954102012000314>
- Carmona, E., Almendros, J., Peña, J. A., & Ibáñez, J. M. (2010). Characterization of fracture systems using precise array locations of earthquake multiplets: An example at Deception Island volcano, Antarctica. *Journal of Geophysical Research*, 115, B06309. <https://doi.org/10.1029/2009JB006865>
- Catalán, M., Galindo-Zaldívar, J., Martín-Dávila, J., Martos, Y. M., Maldonado, A., Gamboa, L., & Schreider, A. A. (2013). Initial stages of oceanic spreading in the Bransfield Rift from magnetic and gravity data analysis. *Tectonophysics*, 585, 102–112. <https://doi.org/10.1016/j.tecto.2012.09.016>
- Catalán, M., Martos, Y. M., Galindo-Zaldívar, J., & Funaki, M. (2014). Monitoring the evolution of Deception Island volcano from magnetic anomaly data (South Shetland Islands, Antarctica). *Global and Planetary Change*, 123(Part B), 199–212. <https://doi.org/10.1016/j.gloplacha.2014.07.018>
- Christeson, G. L., Barker, D. H. N., Austin, J. A., & Dalziel, I. W. D. (2003). Deep crustal structure of Bransfield Strait: Initiation of a back arc basin by rift reactivation and propagation. *Journal of Geophysical Research*, 108(B10), 2492. <https://doi.org/10.1029/2003JB002468>
- Coulon, C., Hsieh, P., White, R., Lowenstern, J., & Ingebritsen, S. (2017). Causes of distal volcano-tectonic seismicity inferred from hydrothermal modeling. *Journal of Volcanology and Geothermal Research*, 345, 98–108. <https://doi.org/10.1016/j.jvolgeores.2017.07.011>
- Díaz-Moreno, A., Ibáñez, J. M., De Angelis, S., García-Yeguas, A., Prudencio, J., Morales, J., et al. (2015). Seismic hydraulic fracture migration originated by successive deep magma pulses: The 2011–2013 seismic series associated to the volcanic activity of El Hierro island. *Journal of Geophysical Research: Solid Earth*, 120, 7749–7770. <https://doi.org/10.1002/2015JB012249>
- Dietrich, R., Rulke, A., Ihde, J., Lindner, K., Miller, H., Niemeier, W., et al. (2004). Plate kinematics and deformation status of the Antarctic Peninsula based on GPS. *Global and Planetary Change*, 42(1), 313–321. <https://doi.org/10.1016/j.gloplacha.2003.12.003>
- Dziak, R. P., Park, M., Lee, W. S., Matsumoto, H., Bohnenstiehl, D. R., & Haxel, J. H. (2010). Tectonomagmatic activity and ice dynamics in the Bransfield Strait back-arc basin, Antarctica. *Journal of Geophysical Research*, 115, B01102. <https://doi.org/10.1029/2009JB006295>
- Freed, A. M. (2005). Earthquake triggering by static, dynamic, and postseismic stress transfer. *Annual Review of Earth and Planetary Sciences*, 33(1), 335–367. <https://doi.org/10.1146/annurev.earth.33.092203.122505>
- Gabrieli, A., Wilson, L., & Lane, S. (2015). Volcano-tectonic interactions as triggers of volcanic eruptions. *Proceedings of the Geologists Association*, 126(6), 675–682. <https://doi.org/10.1016/j.pgeola.2015.10.002>
- Galindo-Zaldívar, J., Gamboa, L., Maldonado, A., Nakao, S., & Bochu, Y. (2004). Tectonic development of the Bransfield Basin and its prolongation to the South Scotia Ridge, northern Antarctic Peninsula. *Marine Geology*, 206(1-4), 267–282. <https://doi.org/10.1016/j.margeo.2004.02.007>
- García-Yeguas, A., Almendros, J., Abella, R., & Ibáñez, J. M. (2011). Quantitative analysis of seismic wave propagation anomalies in azimuth and apparent slowness at Deception Island volcano (Antarctica) using seismic arrays. *Geophysical Journal International*, 184, 801–815. <https://doi.org/10.1111/j.1365-246X.2010.04864.x>
- Gracia, E., Canals, M., Farran, M.-L., Prieto, M. J., Sorribas, J., & Team, GEBRA (1996). Morphostructure and evolution of the central and eastern Bransfield Basins (NW Antarctic Peninsula). *Marine Geophysical Research*, 18(2-4), 429–448. <https://doi.org/10.1007/BF00286088>

- Grad, M., Shiobara, H., Janik, T., Guterch, A., & Shimamura, H. (1997). Crustal model of the Bransfield Rift, West Antarctica, from detailed OBS refraction experiments. *Geophysical Journal International*, 130(2), 506–518. <https://doi.org/10.1111/j.1365-246X.1997.tb05665.x>
- Harris, A. J. L., & Ripepe, M. (2007). Regional earthquake as a trigger for enhanced volcanic activity: Evidence from MODIS thermal data. *Geophysical Research Letters*, 34, L02304. <https://doi.org/10.1029/2006GL028251>
- Havskov, J., & Alguacil, G. (2016). *Instrumentation in earthquake seismology* (2nd ed.). Dordrecht, Netherlands: Springer. <https://doi.org/10.1007/978-3-319-21314-9>
- Havskov, J., & Ottemoller, L. (1999). SEISAN earthquake analysis software. *Seismological Research Letters*, 70, 532–534.
- Havskov, J., & Ottemoller, L. (2010). *Routine data processing in earthquake seismology: With sample data, exercises and software*. Dordrecht, Netherlands: Springer.
- Havskov, J., Peña, J. A., Ibáñez, J. M., Ottemoller, L., & Martínez-Arévalo, C. (2003). Magnitude scales for very local earthquakes. Application for Deception Island volcano (Antarctica). *Journal of Volcanology and Geothermal Research*, 128(1-3), 115–133. [https://doi.org/10.1016/S0377-0273\(03\)00250-6](https://doi.org/10.1016/S0377-0273(03)00250-6)
- Hill, D. P. (2008). Dynamic stresses, Coulomb failure and remote triggering. *Bulletin of the Seismological Society of America*, 98, 66–92. <https://doi.org/10.1785/0120120085>
- Hill, D. P., Pollitz, F., & Newhall, C. (2002). Earthquake-volcano interactions. *Physics Today*, 55(11), 41–47. <https://doi.org/10.1063/1.1535006>
- Hill, D., & Prejean, S. (2015). Dynamic triggering (2nd ed.). In G. Schubert & H. Kanamori (Eds.), *Earthquake seismology, treatise on geophysics* (Vol. 4, chap. 11, pp. 273–304). Elsevier. <https://doi.org/10.1016/B978-0-444-53802-4.00078-6>
- Hill, D. P., Reasenber, P. A., Michael, A., Arabaz, W. J., Beroza, G., Brumbaugh, D., et al. (1993). Seismicity remotely triggered by the magnitude 7.3 Landers, California, Earthquake. *Science*, 260(5114), 1617–1623. <https://doi.org/10.1126/science.260.5114.1617>
- ISC (2017). On-line bulletin. Retrieved from <http://www.isc.ac.uk>, Internat. Seismol. Cent., Thatcham, UK.
- Ibáñez, J. M., Almendros, J., Carmona, E., Martínez-Arévalo, C., & Abril, M. (2003). The recent seismo-volcanic activity at Deception Island volcano. *Deep Sea Research II*, 50(10-11), 1611–1629. [https://doi.org/10.1016/S0967-0645\(03\)00082-1](https://doi.org/10.1016/S0967-0645(03)00082-1)
- Ibáñez, J. M., Carmona, E., Almendros, J., Saccorotti, G., Del Pezzo, E., Abril, M., & Ortiz, R. (2003). The 1998–1999 seismic series at Deception Island volcano, Antarctica. *Journal of Volcanology and Geothermal Research*, 128(1-3), 65–88. [https://doi.org/10.1016/S0377-0273\(03\)00247-6](https://doi.org/10.1016/S0377-0273(03)00247-6)
- Ibáñez, J. M., Del Pezzo, E., Almendros, J., La Rocca, M., Alguacil, G., Ortiz, R., & García, A. (2000). Seismovolcanic signals at Deception Island volcano, Antarctica: Wave field analysis and source modeling. *Journal of Geophysical Research*, 105(B6), 13,905–13,931. <https://doi.org/10.1029/2000JB900013>
- Ibáñez, J. M., Díaz-Moreno, A., Prudencio, J., Zandomenighi, D., Wilcock, W., Barclay, A., et al. (2017). Database of multi-parametric geophysical data from the Tomodec experiment on Deception Island, Antarctica. *Scientific Data*, 4, 170128. <https://doi.org/10.1038/sdata.2017.128>
- Ibáñez, J. M., Morales, J., Alguacil, G., Almendros, J., Ortiz, R., & Del Pezzo, E. (1997). Intermediate-focus earthquakes under South Shetland Islands, Antarctica. *Geophysical Research Letters*, 24(5), 531–534. <https://doi.org/10.1029/97GL00314>
- Jiménez, V., Almendros, J., & Carmona, E. (2017). Detection of long-duration tremors at Deception Island volcano, Antarctica. *Journal of Volcanology and Geothermal Research*, 347, 234–249. <https://doi.org/10.1016/j.jvolgeores.2017.09.016>
- Johnston, M. J. S., Prejean, S. G., & Hill, D. P. (2004). Triggered deformation and seismic activity under Mammoth Mountain in Long Valley caldera by the 3 November 2002 M_w 7.9 Denali Fault earthquake. *Bulletin of the Seismological Society of America*, 94(6B), S360–S369. <https://doi.org/10.1785/0120040603>
- Kisslinger, C., & Jones, L. M. (1991). Properties of aftershock sequences in Southern California. *Journal of Geophysical Research*, 96(B7), 11,947–11,958. <https://doi.org/10.1029/91JB01200>
- LeMasurier, W. E., & Thomson, J. W. (Eds.) (1990). Volcanoes of the Antarctic plate and southern Oceans. In *Antarctic Research Series* (Vol. 48, pp. 1–487). Washington, DC: American Geophysical Union.
- Lemarchand, N., & Grasso, J.-R. (2007). Interactions between earthquakes and volcano activity. *Geophysical Research Letters*, 34, L24303. <https://doi.org/10.1029/2007GL031438>
- Lienert, B. R. E., & Havskov, J. (1995). A computer program for locating earthquakes both locally and globally. *Seismological Research Letters*, 66, 26–36.
- Linde, A. T., & Sacks, I. S. (1998). Triggering of volcanic eruptions. *Nature*, 395(6705), 888–890. <https://doi.org/10.1038/27650>
- Luzón, F., Almendros, J., & García-Jerez, A. (2011). Shallow structure of Deception Island, Antarctica, from correlations of ambient seismic noise on a set of dense seismic arrays. *Geophysical Journal International*, 185, 737–748. <https://doi.org/10.1111/j.1365-246X.2011.04962.x>
- Maldonado, A., Dalziel, I. W. D., & Leat, P. T. (2015). The global relevance of the Scotia Arc: An introduction. *Global and Planetary Change*, 125, A1–A8. <https://doi.org/10.1016/j.gloplacha.2014.06.011>
- Manga, M., & Brodsky, E. (2006). Seismic triggering of eruptions in the far field: Volcanoes and geysers. *Annual Review of Earth and Planetary Sciences*, 34, 263–291. <https://doi.org/10.1146/annurev.earth.34.031405.125125>
- Martí, J., Geyer, A., & Aguirre-Díaz, G. (2013). Origin and evolution of the Deception Island caldera (South Shetland Islands, Antarctica). *Bulletin of Volcanology*, 75, 1–18. <https://doi.org/10.1007/s00445-013-0732-3>
- Marzocchi, W. (2002). Remote seismic influence on large explosive eruptions. *Journal of Geophysical Research*, 107(B1), 2018. <https://doi.org/10.1029/2001JB000307>
- Nishimura, T. (2017). Triggering of volcanic eruptions by large earthquakes. *Geophysical Research Letters*, 44, 7750–7756. <https://doi.org/10.1002/2017GL074579>
- Ortiz, R., García, A., Aparicio, A., Blanco, I., Felpeto, A., Del-Rey, R., et al. (1997). Monitoring of the volcanic activity of Deception Island, South Shetland Islands, Antarctica (1986–1995). In C. A. Ricci (Ed.), *The Antarctic region: Geological evolution and processes* (pp. 1071–1076). Siena, Italy: Terra Antarctica Publication.
- Pedraza, A., Ruiz-Constan, A., Heredia, N., Galindo-Zaldívar, J., Bohoyo, F., Marin-Lechado, C., et al. (2012). The fracture system and the melt emplacement beneath the Deception Island active volcano, South Shetland Islands, Antarctica. *Antarctic Science*, 24, 173–182. <https://doi.org/10.1017/S0954102011000794>
- Pelayo, A. M., & Wiens, D. A. (1989). Seismotectonics and relative plate motions in the Scotia Sea region. *Journal of Geophysical Research*, 94(B6), 7293–7320. <https://doi.org/10.1029/JB094iB06p07293>
- Prejean, S. G., Hill, D. P., Brodsky, E. E., Hough, S. E., Johnston, M. J. S., Malone, S. D., et al. (2004). Remotely triggered seismicity on the United States West Coast following the $M7.9$ Denali fault earthquake. *Bulletin of the Seismological Society of America*, 94(6B), S348–S359. <https://doi.org/10.1785/0120040610>
- Prudencio, J., De Siena, L., Ibáñez, J. M., Del Pezzo, E., García-Yeguas, A., & Díaz-Moreno, A. (2015). The 3D attenuation structure of Deception Island (Antarctica). *Surveys in Geophysics*, 36(3), 371–390. <https://doi.org/10.1007/s10712-015-9322-6>

- Prudencio, J., Ibáñez, J. M., García-Yeguas, A., Del Pezzo, E., & Posadas, A. M. (2013). Spatial distribution of intrinsic and scattering seismic attenuation in active volcanic islands, II: Deception Island images. *Geophysical Journal International*, *195*(3), 1957–1969. <https://doi.org/10.1093/gji/ggt360>
- Roberts, N. S., Bell, A. F., & Main, I. G. (2015). Are volcanic seismic *b*-values high, and if so when? *Journal of Volcanology and Geothermal Research*, *308*, 127–141. <https://doi.org/10.1016/j.jvolgeores.2015.10.021>
- Robertson-Maurice, S. D., Wiens, D. A., Shore, P. J., Vera, E., & Dorman, L. M. (2003). Seismicity and tectonics of the South Shetland Islands and Bransfield Strait from a regional broadband seismograph deployment. *Journal of Geophysical Research*, *108*(B10), 2461. <https://doi.org/10.1029/2003JB002416>
- Rundquist, D., & Sobolev, P. (2002). Seismicity of mid-oceanic ridges and its geodynamic implications: A review. *Earth-Science Reviews*, *58*(1), 143–161. [https://doi.org/10.1016/S0012-8252\(01\)00086-1](https://doi.org/10.1016/S0012-8252(01)00086-1)
- Ryan, W. B. F., Carbotte, S. M., Coplan, J. O., O'Hara, S., Melkonian, A., Arko, R., et al. (2009). Global multi-resolution topography synthesis. *Geochemistry, Geophysics, Geosystems*, *10*, Q03014. <https://doi.org/10.1029/2008GC002332>
- Saccorrotti, G., Ventura, G., & Vilardo, G. (2002). Seismic swarms related to diffusive processes: The case of Somma-Vesuvius volcano, Italy. *Geophysics*, *67*(1), 199–203. <https://doi.org/10.1190/1.1451551>
- Shearer, P. M. (2009). *Introduction to seismology* (2nd ed.). New York: Cambridge University Press.
- Smellie, J. L. (2002). The 1969 subglacial eruption on Deception Island (Antarctica): Events and processes during an eruption beneath a thin glacier and implications for volcanic hazards. In J. L. Smellie & M. G. Chapman (Eds.), *Volcano-ice interaction on Earth and Mars, special publications* (Vol. 202, pp. 59–79). Geological Society of London. <https://doi.org/10.1144/GSL.SP.2002.202.01.04>
- Steady, S., Gombert, J., & Cocco, M. (2005). Introduction to special section: Stress transfer, earthquake triggering, and time-dependent seismic hazard. *Journal of Geophysical Research*, *110*, B05S01. <https://doi.org/10.1029/2005JB003692>
- Stich, D., Almendros, J., Jiménez, V., Mancilla, F., & Carmona, E. (2011). Ocean noise triggering of rhythmic long period events at Deception Island volcano. *Geophysical Research Letters*, *38*, L22307. <https://doi.org/10.1029/2011GL049671>
- Utheim, T., Havskov, J., Ozyazicioglu, M., Rodriguez, J., & Talavera, E. (2014). Rtquake, a real-time earthquake detection system integrated with Seisan. *Seismological Research Letters*, *85*(3), 735–742. <https://doi.org/10.1785/0220130175>
- Utsu, T., Ogata, Y., & Matsu'ura, R. S. (1995). The centenary of the Omori formula for a decay law of aftershock activity. *Journal of Physics of the Earth*, *43*(1), 1–33. <https://doi.org/10.4294/jpe1952.43.1>
- van der Elst, T., & Brodsky, E. E. (2010). Connecting near-field and far-field earthquake triggering to dynamic strain. *Journal of Geophysical Research*, *115*, B07311. <https://doi.org/10.1029/2009JB006681>
- Vassallo, M., Satriano, C., & Lomax, A. (2012). Automatic picker developments and optimization: An optimization strategy for improving the performance of automatic phase pickers. *Seismological Research Letters*, *83*(3), 541–554. <https://doi.org/10.1785/gssrl.83.3.541>
- Walter, T., Wang, R., Acocella, V., Neri, M., Grosser, H., & Zschau, J. (2009). Simultaneous magma and gas eruptions at three volcanoes in Southern Italy: An earthquake trigger? *Geology*, *37*(3), 251–254. <https://doi.org/10.1130/G25396A>
- Walter, T. R., Wang, R., Zimmer, M., Grosser, H., Luhr, B., & Ratdomopurbo, A. (2007). Volcanic activity influenced by tectonic earthquakes: Static and dynamic stress triggering at Mt. Merapi. *Geophysical Research Letters*, *34*, L05304. <https://doi.org/10.1029/2006GL028710>
- Weber, B., Becker, J., Hanka, W., Heinloo, A., Hoffmann, M., Kraft, T., et al. (2007). Seiscomp3—Automatic and interactive real time data processing. *Geophysical Research Abstracts* (Vol. 9, No. 09219). Vienna: EGU General Assembly.
- White, R., & McCausland, W. (2016). Volcano-tectonic earthquakes: A new tool for estimating intrusive volumes and forecasting eruptions. *Journal of Volcanology and Geothermal Research*, *309*, 139–155. <https://doi.org/10.1016/j.jvolgeores.2015.10.020>
- Zandomenighi, D., Barclay, A., Almendros, J., Ibáñez, J. M., Wilcock, W. S. D., & Ben-Zvi, T. (2009). Crustal structure of Deception Island volcano from *P* wave seismic tomography: Tectonic and volcanic implications. *Journal of Geophysical Research*, *114*, B06310. <https://doi.org/10.1029/2008JB006119>